EXPERIMENTAL CELL RESEARCH 317 (2011) 1979–1993

available at www.sciencedirect.com

ScienceDirect

www.elsevier.com/locate/yexcr

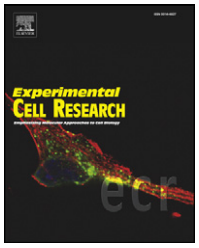

Research Article

The isolated muscle fibre as a model of disuse atrophy: Characterization using PhAct, a method to quantify f-actin

*William J. Duddy**, *Tatiana Cohen*, *Stephanie Duguez*, *Terence A. Partridge*

Center for Genetic Medicine, Children's Research Institute, Children's National Medical Center, Washington DC, USA

ARTICLE INFORMATION

Article Chronology:
Received 18 December 2010
Revised version received 8 April 2011
Accepted 13 May 2011
Available online 20 May 2011

Keywords:
Muscle atrophy
Myofibre
Myonucleus
Myoblast
Myostatin
Follistatin

ABSTRACT

Research into muscle atrophy and hypertrophy is hampered by limitations of the available experimental models. Interpretation of *in vivo* experiments is confounded by the complexity of the environment while *in vitro* models are subject to the marked disparities between cultured myotubes and the mature myofibres of living tissues. Here we develop a method (PhAct) based on *ex vivo* maintenance of the isolated myofibre as a model of disuse atrophy, using standard microscopy equipment and widely available analysis software, to measure f-actin content per myofibre and per nucleus over two weeks of *ex vivo* maintenance. We characterize the 35% per week atrophy of the isolated myofibre in terms of early changes in gene expression and investigate the effects on loss of muscle mass of modulatory agents, including Myostatin and Follistatin. By tracing the incorporation of a nucleotide analogue we show that the observed atrophy is not associated with loss or replacement of myonuclei. Such a completely controlled investigation can be conducted with the myofibres of a single muscle. With this novel method we can distinguish those features and mechanisms of atrophy and hypertrophy that are intrinsic to the muscle fibre from those that include activities of other tissues and systemic agents.

Introduction

Methods for the isolation and *ex vivo* maintenance of intact single myofibres have been known for some years [1,2]. The isolated muscle fibre has proved useful in the study of satellite cell behaviour *ex vivo*[3] and *in vivo*[4] but the cell biology of the myofibre itself has largely been neglected. Atrophy of the myofibre is an important component of numerous human conditions, including aging, bed-rest, sepsis, and many neuromuscular disorders, and loss of muscle mass is a risk factor for post-operative morbidity (reviewed [5]).

Changes in muscle mass in the living animal have been assessed by a range of methods from gross measurements of whole muscle protein content [6–9] or inferences from muscle cross-sections [10–12], to low-throughput intensive analyses of confocalized z-stacks [13]. Such investigations are labor- and animal-intensive, largely restricting investigation to very specific mechanisms or modulatory agents. Moreover, because of the

* *Corresponding author.*
E-mail addresses: bduddy@cnmcresearch.org (W.J. Duddy), tcohen@cnmcresearch.org (T. Cohen), sduguez@cnmcresearch.org (S. Duguez), tpartridge@cnmcresearch.org (T.A. Partridge).

Abbreviations: EdU, 5-ethynyl-2′-deoxyuridine; EDL, Extensor Digitorum Longus; SDS-PAGE, sodium dodecyl sulfate polyacrylamide gel electrophoresis; MuRF-1, Muscle RING-finger protein-1; Eif4ebp1, PHAS-1, Eukaryotic translation initiation factor 4E-binding protein 1; eIF-4E, Eukaryotic translation initiation factor 4E; NF-κB, nuclear factor kappa-light-chain-enhancer of activated B cells; TNFα, Tumor necrosis factor-alpha; IL-1, Interleukin-1 alpha

0014-4827/$ – see front matter © 2011 Elsevier Inc. All rights reserved.
doi:10.1016/j.yexcr.2011.05.013

complexity of the biological control of muscle size in the whole animal, they are necessarily empirical in nature and cannot be used to rigorously investigate specific mechanisms. A second general approach has been to extrapolate from the behaviour of *in vitro* cultures of myotubes [14–16]. The less intensive of these methods are generally inadequate to determine change in the volume of cytoplasm served by each myonucleus, the size of the myonuclear domain (MND). Loss of MND size is a near-universal observation following *in vivo* atrophy [13,17–27], and is usually determined by combination of the methods above with counts of myonuclei per millimeter of myofibre, itself a method not immune to error, since it does not take account of myofibre length.

Various compounds are shown or suggested to influence myofibre size, some of which potentially affect the rate of atrophy. The Activin type II receptor agonist, Myostatin, a negative regulator of muscle mass [28], and its inhibitor Follistatin [29] are of major current interest, on the expectation that increased muscle mass resulting from the inhibition of myostatin activity might protect against atrophic stimuli. Putative positive regulators of muscle mass include the insulin-like growth factor, IGF-1 (reviewed [30]), and the metabolite, Leucine [31]. The study of muscle mass regulation is limited by current models because of the complexity of the *in vivo* muscle environment and the questionable relationship of *in vitro* tissue culture to the *in vivo* system.

Here the *ex vivo* maintenance of the isolated myofibre is evaluated as a potential tool for the study of atrophy induced by denervation and lack of work. We propose that it represents a model intermediate between *in vivo* and *in vitro* approaches in that the atrophic environment may be carefully controlled whilst retaining much of the phenotypic character of living muscle tissue. A further advantage is the reduction of animal requirements, since a fully controlled experiment may be conducted with the myofibres from a single muscle. We present a novel method for the sensitive measurement of contractile actin content per myofibre that when combined with counts of nuclei per myofibre gives the f-actin content per nucleus, an indicator of the myonuclear domain size. We call this method PhAct, a contraction of Phalloidin-based Actin quantification. Atrophy-associated myonuclear loss is assayed in myofibres isolated from the extensor digitorum longus (EDL) muscles of transgenic mice expressing a myonuclear marker. Incorporation of the nucleotide analogue, 5-ethynyl-2′-deoxyuridine (EdU), is used to investigate myonuclear accretion or replacement during atrophy. Early changes in gene expression are characterized, and the effects on the rate of atrophy induced by several putative regulators of muscle mass (Myostatin, Follistatin, and Leucine) are measured.

Materials and methods

Animal use

Two mouse lines were used in this study: wild-type C57BL/10SnJ (JAX Mice), and the transgenic strain 3F-nLacZ-e (M. Buckingham). The 3F-nLacZ-e mouse is on a C57BL/6 X SJL background and expresses LacZ protein driven from a myonuclear specific promoter, myosin light chain type 3F [32]. Three-month old male mice were used as by this age the EDL muscle has attained full adult size and provides a stable basis for comparison of rates of atrophy in response to a given treatment. Sufficient myofibres were isolated from a single animal by pooling myofibres from the two EDL muscles for each experiment, except for analysis of gene expression, for which three animals were used per time-point and a single sample of 180 myofibres was collected from each animal. All animal procedures were performed according to Children's National Medical Center Institutional Animal Care and Use Committee, and National Institutes of Health guidelines.

Isolation of myofibres

Reagents were from Invitrogen unless otherwise stated. Single myofibres were isolated as described previously [3]. Briefly: extensor digitorum longus (EDL) muscles were carefully dissected immediately after euthanasing the mouse and incubated in 0.2% Collagenase Type 1 (Sigma) in DMEM for 1 to 2 h, depending on muscle size, to digest the connective tissue. Single myofibres were liberated by trituration with fire-smoothed wide-mouthed Pasteur pipettes in dishes containing DMEM and pre-coated with horse serum (to prevent adherence); liberated myofibres were washed by transfer through four such dishes.

Ex vivo maintenance and treatment of myofibres

Isolated myofibres were maintained in free-floating suspension in deep-sided dishes (Sterilin) coated with horse serum and containing DMEM (with 4500 mg/L D-glucose, L-glutamine, and 110 mg/L sodium pyruvate) with the following additional components: 10% v/v horse serum, 2% v/v (4 mM) L-glutamine (Sigma), and 1% v/v Penicillin/Streptomycin (Sigma). Twenty-five myofibres were placed in each dish. Half of the medium was removed and replaced with fresh medium every 3 days in culture. Dishes were swirled briefly in a gentle circular motion once per day to guard against tangling of myofibres.

Test compounds were added directly to the culture medium at various concentrations daily or every three days, as listed in the results section: Recombinant Mouse Follistatin (R & D systems), Recombinant Mouse GDF-8/Myostatin (R & D systems), and Leucine (Sigma).

Fixation and staining of myofibres for assay of f-actin content and counting of nuclei

Batches of myofibres were harvested at each time-point by transferring them to a 2 ml Eppendorf vial containing 1.5 ml 3.65% Formaldehyde, in which they were fixed at 37 °C for 15 min. The vial was centrifuged at 700 g for 10 min, causing the myofibres to form a loose pellet, delicately attached to the bottom of the vial. The formaldehyde solution was removed carefully with a Pasteur pipette so as not to disturb the pellet then 1 ml of 30% sucrose was added. The myofibres were resuspended using a brief (3 s) vortex then stored at −80 °C until staining.

The Eppendorf vial containing fixed myofibres in 30% sucrose was allowed to thaw and the contents were deposited into a Petri dish. To ensure that all of the myofibres were removed from the Eppendorf it was rinsed once with a solution of TBS-tween (Tween 0.1% in TBS) which was deposited into the same Petri dish. Because the density of the sucrose prevented pelleting of the fibers we used a stereo microscope and watchmakers forceps to transfer myofibres carefully into a 2 ml Eppendorf vial containing permeabilization and blocking buffer (Triton 0.5%, Tween 0.1%, BSA 2%,

and Goat serum 20%, in TBS-tween). After an overnight incubation at 4 °C the vial was centrifuged for 10 min at 15,000 *g*. The buffer was removed and 1 ml of rinse solution (TBS-tween) was added. The myofibres were resuspended with a brief (3 sec) vortex, then centrifuged for a further 10 min at 15,000 *g*. This rinse step was repeated 3 times. Myofibres were then resuspended in Alexa Fluor 594 conjugated Phalloidin for 20 min at room temperature at a dilution of 1:40 unless otherwise stated. After 3 more rinses the fibres were left in the rinse solution overnight at 4 °C to maximize removal of unbound Phalloidin. After centrifugation for 10 minutes at 15,000 *g*, myofibres were resuspended in a 0.75 μg/ml solution of DAPI and immediately centrifuged a further 10 min at 15,000 *g*, then rinsed once more. The contents of the vial were deposited into a Petri dish and the vial was rinsed once to ensure removal of all myofibres from the Eppendorf. A stereo microscope and forceps were used to transfer the myofibres gently onto a microscope slide on which they were mounted.

Imaging and software analysis

Stained myofibres were imaged on standard epifluorescence microscopy equipment: a Nikon Eclipse E500 microscope with Spot Camera. A Nikon PlanApo 10× objective was used to image adjacent overlapping segments of each myofibre. Between 2 and 6 images were required, depending on the length of the myofibre. Initially, exposure time was set to fall within a range of signal intensity that was validated to elicit a linear response in measured signal. Exposure time was then kept constant across all samples compared.

Images of the myofibre were stitched together using the'Interactive Layout' mode of the Photomerge feature of Adobe Photoshop. Interactive layout is the default mode for Adobe Photoshop version CS2 and is available in current versions of Adobe Photoshop Elements, but is absent from some later versions of Adobe Photoshop such as CS4, for which a 'PhotomergeUI' plug-in, from Adobe, may be required. The 'Snap to image' feature of the Interactive Layout mode was found to respond best to color-inverted images (i.e. presenting the myofibre on a white background as opposed to the black background of the original image).

The total signal intensity of stitched images was measured using ImageJ (http://rsbweb.nih.gov/ij/). Each image was uninverted following stitching in Photoshop, and then converted into a 32-bit image. Lower threshold for pixel quantification was set to '1' to eliminate background pixels, with non-thresholded pixels set to the NaN (Not a Number) value, and then the integrated density (total signal) of the image was quantified. An imageJ Macro named 'PhAct' was created to facilitate batch operations of the above steps on multiple images (http://rsbweb.nih.gov/ij/macros/).

For confocal microscopy, z-stacks were acquired using a Zeiss LSM 510 Meta NLO system with an Axiovert 200 M microscope. Depths ranged from 35.3 to 61.8 μm, depending on myofibre thickness. Slices 2.2 μm thick composed of 512 by 512 pixels were collected with 20× objective. Between 2 and 6 non-adjacent z-stacks were collected per myofibre, depending on myofibre length. DAPI-stained nuclei were counted for each z-stack by eye from 3D representation using Axiovision software (Zeiss) and added together for each myofibre. ImageJ was used to calculate the integrated density of signal from Fluorophore-conjugated Phalloidin for each slice, which were added together to give total signal per z-stack. Signals per z-stack were added for each myofibre and divided by the number of nuclei to give signal per nucleus, which was normalized to the average signal per nucleus of the myofibres from 28 week old mice.

Confirmation of equipment sensitivity and consistency

A 10 μl drop of fluorophore conjugated Phalloidin of fixed concentration (1:4 in H_2O) was used as a standard signal. Imaging of this at various exposure times confirmed that measured signal increased in linear proportion to actual signal. Averages of four images were taken per exposure time . ImageJ was used to calculate the mean pixel intensity for each field. A minor adjustment is made to measurements of signal intensity according to the y-intercept of the plot of mean pixel intensity against exposure time. Imaging of this standard signal can be used to normalize data across different experimental series.

Measurement of protein content of isolated myofibres

To investigate the extent to which f-actin protein content is reflective of total protein content, total protein was measured on batches of twenty myofibres by quantifying silver stain intensities of whole protein extracts separated out by SDS-PAGE. We compared batches at two time-points (Day 0 and Day 9). Silver stain was chosen due to its greater sensitivity over others such as Coomassie Blue. Briefly, isolated myofibres were placed in protein extraction buffer (NaCl 300 mM, NaH_2PO_4 100 mM, Na_2HPO_4 50 mM, $Na_4P_2O_7$ 10 mM, $MgCl_2 \times 6H_2O$ 1 mM, EDTA 10 mM, 2-β-mercaptoethanol 0.7% (Sigma), with protease inhibitor cocktail according to manufacturer's instructions (Roche)) and stored at −20 °C. Samples were homogenized by freezing and thawing three times, treated with DNase, and passed through a fine-gauge syringe. For loading, two parts sample were mixed with two parts glycerol and one part loading buffer (NuPage 4× + 50 mM DTT, Sigma). Polyacrylamide gel (8%) was run for 55 min at 150 V in MOPS buffer. Gels were silver stained according to manufacturer's instructions (Sigma) and imaged. Analysis was carried out using ImageJ. All bands were quantified except the one corresponding to serum albumin (60 kDa), a contaminant from the myofibre isolation procedure.

Immunostaining of myonuclei and adherent cell nuclei, and labeling of proliferating nuclei

To immunostain myonuclei and adherent cell nuclei myofibres were incubated with primary antibodies for 2 h at room temperature following the permeabilization and blocking step then rinsed 3 times and incubated with secondary antibodies for 1 h at room temperature followed by 2 rinses and one overnight rinse step to minimize non-specific background staining of myofibres. Myonuclei of myofibres isolated from the 3F-nLacZ-e mouse were immunostained using Rabbit IgG Anti β-Galactosidase primary antibody (1:300 dilution) and Alexa Fluor 594 anti-rabbit secondary antibody (1:400 dilution). Myonuclei were immunostained using a mixture of two mouse IgG1 primary antibodies, anti-Pax7 (Developmental Studies Hybridoma Bank; undiluted) and anti-MyoD (Vector labs; 1:25 dilution), and the Alexa Fluor-488 anti-mouse IgG1 secondary (1:400 dilution). This co-stain marks both quiescent (Pax7 expressing) and activated (MyoD expressing) myoblasts.

To mark nuclei that undergo proliferation events, myofibres were maintained in culture in the presence of the nucleotide analogue, 5-ethynyl-2′-deoxyuridine (EdU). DNA containing EdU was labeled using the Click-iT EdU Alexa Fluor 594 Imaging Kit, and adapting from the manufacturer's instructions. The method was similar to that described for the staining of f-actin using Phalloidin, except that myofibres were permeabilized with 0.5% Triton in PBS for 20 min at room temperature, then incubated with the EdU Click-iT reaction cocktail for 30 min at room temperature prior to the overnight permeabilization and blocking step.

Microarray mRNA expression profiling and quantitative real-time PCR

RNA was extracted from triplicate batches of 180 isolated myofibres at days 0, 1, and 2, of *ex vivo* culture. Myofibres were placed into culture medium contained in BSA-coated round-bottomed glass vials and allowed to settle for 2 min at the bottom of the vial. Medium was then replaced by 1 ml of Trizol, in which the myofibres were triturated by 50 passes through a 1 ml pipette tip. Each batch was then stored at −80 °C prior to purification on RNeasy spin columns (Qiagen). Approximately 120 ng of total RNA was obtained from each batch of 180 myofibres. Total RNA was amplified (two-cycle) and hybridized to Affymetrix GeneChip Mouse Expression Set 430 2.0 according to the manufacturer's instructions (Affymetrix USA). Gene expression data analysis was performed using the probe set algorithms MAS5.0 and dCHIP and data visualization and statistical analyses using GeneSpring Software (Stratagene). Hierarchical Clustering Analysis showed clustering of batches in accordance with time-points (data not shown). Candidate probe sets showing changes between time-points were selected based upon their concordance in MAS5.0 and dChip algorithms with a Welch ANOVA *t*-test of $p < 0.05$ compared with day 0.

Fifty-six mRNA transcripts of interest were selected and confirmed by RT-PCR. Samples independent from gene profiling experiments were used for validation studies. Total RNA was isolated as above and 22 ng of total RNA was used with 1st Strand cDNA Synthesis Kit (Roche) to generate cDNA. The cDNA was added to SYBR Green PCR Master Mix (Applied Biosystems) and real time PCR was performed using the 7900 HT Fast Real Time PCR system (Applied Biosystems) in the relative quantification ΔΔct mode. Data was analyzed using manufacturer supplied SDS2.3 software.

Statistical analyses

Student's *T*-test was used throughout unless otherwise stated. Figure captions indicate p-values and 95% confidence intervals. Linear regressions are shown where f-actin signal is plotted against number of nuclei or average signal per nucleus is plotted against concentration of phalloidin.

Results

A novel method (PhAct) using phalloidin-staining to quantify f-actin content per myofibre

We wished to determine whether atrophic changes are manifested in isolated single myofibres maintained in tissue culture *ex vivo*, and whether those changes are associated with loss or gain of myonuclei. We hypothesized that f-actin content would decline with *ex vivo* culture time, while myonuclear number would remain unchanged, together reflecting a reduction in size of the myonuclear domain. To test these hypotheses we developed a microscopy-based method whereby f-actin content is quantified

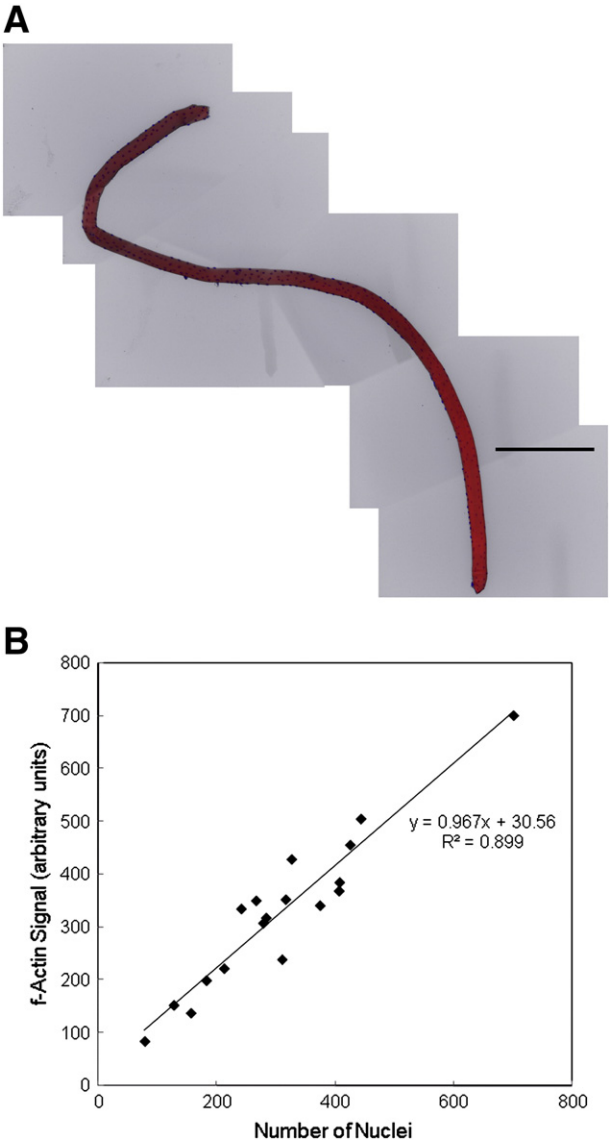

Fig. 1 – Assay of f-actin content using the PhAct method. (A) Micrograph collage of a representative isolated myofibre. Signal from f-actin-bound Alexa Fluor 594 conjugated Phalloidin is shown in red. For illustrative purposes this is merged with DAPI stained nuclei shown in blue and with transmitted light images. Overlapping fields were stitched together to facilitate quantification of whole myofibre f-actin content. Scale bar = 500 μm. (B) The linear relationship of f-actin content to number of nuclei per myofibre. Each datum represents a single myofibre from the EDL muscle of a 3 month-old wild-type mouse. Whole myofibre f-actin content is measured as a relative quantity so units are arbitrary, as described in the Materials and Methods.

and nuclei per myofibre are counted (Fig. 1A). Myofibres were isolated from the EDL muscles of 3 month old male Bl10 mice, at which age, growth has ceased.

We find a directly proportional relationship between the total f-actin signal per myofibre and the number of nuclei per myofibre (Fig. 1B), such that a doubling of nuclear number is associated with an approximate doubling of actin signal. This relationship is consistent with previous reports in suggesting that, within the adult mouse EDL muscle, average myonuclear domain size does not vary greatly between myofibres [33].

We chose a concentration (1:40 dilution, or 0.025 v/v) of fluorophore-conjugated Phalloidin that did not saturate measured signal intensities (Fig. 2A). A validation of the method requires that the microscopy equipment is equally sensitive at all values of fluorescence intensity, within the range of values exhibited by the stained myofibres. Intensity values from myofibres at the exposure time (50 ms) and Phalloidin concentration (1:40) used were in the range 6–10 units per pixel. We show that the measured signal was linear across a range of exposure times of a solution of fluorophore-conjugated Phalloidin within the range 3–14 units per pixel (Fig. 2B). No measurable bleaching occurred between exposures (data not shown).

To further validate the epifluorescence microscopy method we present here we compared values with those obtained from confocal z-stacks. With the standard epifluorescent microscope loss of signal may arise due to portions of the sample lying outside

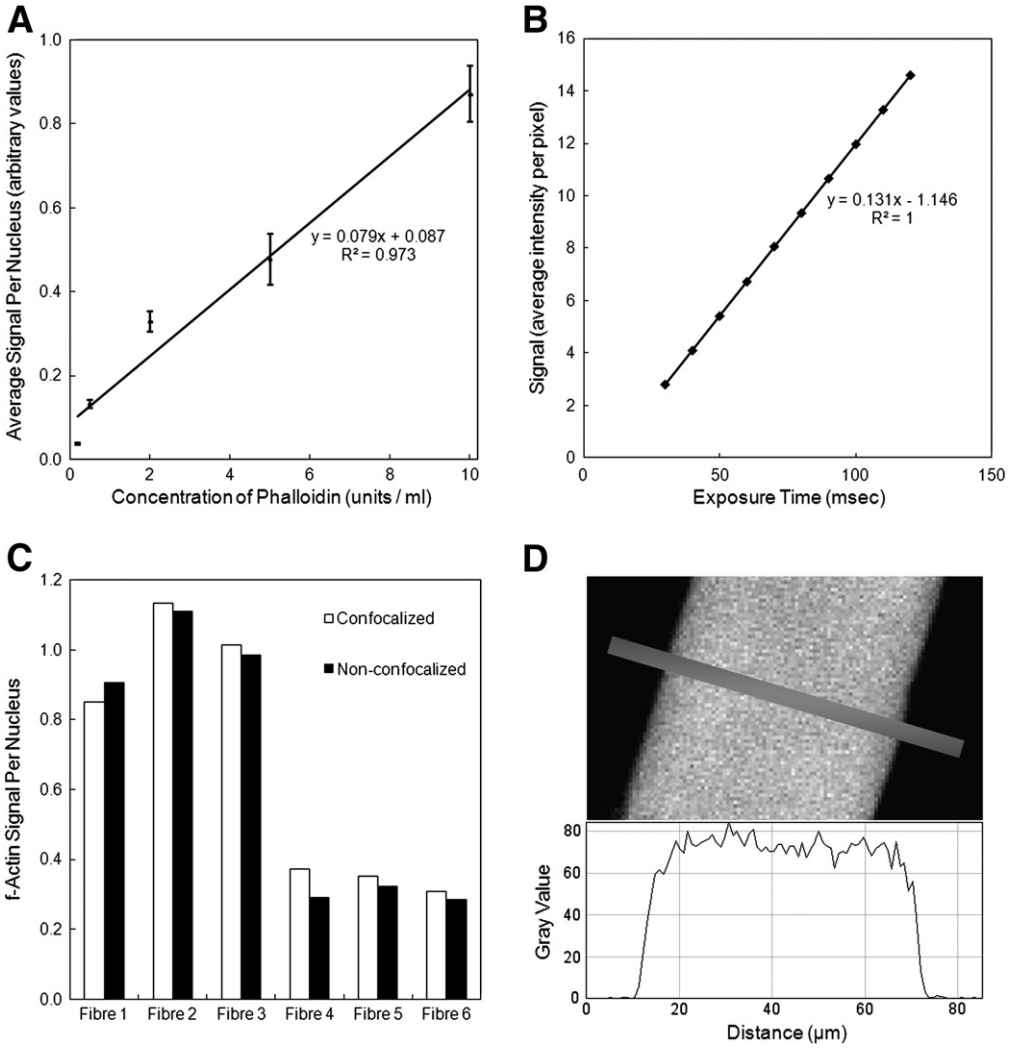

Fig. 2 – Validation of PhAct method. (A) Average ratios of f-actin signal per nucleus at different concentrations of Phalloidin. Alexa Fluor 594 conjugated Phalloidin is prepared at 300 units / ml according to the manufacturer's instructions, then diluted in PBS with 2% BSA. The relationship is linear for a range of concentrations that includes that used for the experiments described (5 units / ml). For each concentration the signal per nucleus ratios of 4–5 myofibres are averaged. (B) Measured signal is directly proportional to actual signal. Average pixel intensity was measured of a solution of Alexa Fluor 594 conjugated Phalloidin over a range of exposure times. (C) Confocalized signal per nucleus matches well to the non-confocalized signal. Fibres 1 to 3 and 4 to 6 were from the EDL muscles of 28 week old and 2 week old male Bl10 mice, respectively. Relative f-actin signal per nucleus is normalized to the average of the 28 week old myofibres for each data set. (D) Alexa Fluor 594 conjugated Phalloidin penetrates equally throughout the myofibre volume. The upper panel shows a central slice from the z-stack of a representative myofibre, with the gray bar indicating a line section. The lower panel shows signal intensity values along this line section. Signal is not diminished in the core of the myofibre.

the focal plane of the objective which collects light from an uncertain depth of the z-axis. Since confocal microscopy allows accurate definition of the z-axis of the focal plane it is possible to obtain more accurate measurement of signal quantity per sample volume. However, with most designs of confocal microscope, confocal z-stacks require long exposures that bleach the imaged region of the myofibre. This bleaching prevents us from stitching overlapping regions of confocal images to estimate the signal per myofibre. We therefore compared ratios of fluorescent phalloidin signal per nucleus, evaluated on whole myofibres by epifluorescence microscopy and subsequently as sample segments of the same fibers by confocal microscopy. Comparison of two sets of three myofibres from mice of two different ages showed excellent agreement between the two methods (Fig. 2C) (the relationship of age to myofibre f-actin content is being explored more fully in a separate investigation). Confocal z-stacks also showed that the mounting procedure (a standard slide and coverslip) flattens the myofibre, squashing its z-axis into a wide x–y profile. This may contribute to the close agreement of the confocalized with the non-confocalized data, suggesting that the 10X objective used for the non-confocalized data gathers light emitted from the full z-axis depth of the mounted myofibre.

A representative confocal image collected at the z-axis mid-point of a myofibre produces equal signal intensity across the myofibre (Fig. 2D), suggesting that fluorophore-conjugated phalloidin has full access to the core of the myofibre such that f-actin quantity will not be underestimated for myofibres with large cross-sections.

Ex vivo diminution of the myonuclear domain is not associated with loss or replacement of myonuclei

Over two weeks of *ex vivo* maintenance we observe a decline in size of isolated myofibres and decreasing spacing of nuclei (Fig. 3A). Using f-actin signal per nucleus at various time-points following isolation as an indicator of atrophy (Fig. 3B), we observe a drop-off of ~35% per week, similar to that observed for *in vivo* denervation, tenotomization, and hind-limb suspension studies of muscles predominant in type II myofibres [6–8,10,13]. Over this period, the number of nuclei per myofibre remains constant, averaging around 330, with considerable variation between individual myofibres (nuclear number per fibre ranged from less than 100 to over 700). The drop in fibrous actin content was paralleled by a 38% drop-off in total protein content between Day 0 and Day 9 (Fig. 3C).

The single myofibre model consists of both the myofibre and adherent cells, largely quiescent satellite cells. To evaluate the role of this adherent cell component of the system, we isolated myofibres from the transgenic mouse strain MLC3F-LacZ, of which myonuclei express LacZ driven by the promoter of Myosin Light Chain type 3F [32] which permits discrimination between myonuclei and nuclei of adherent cells (Fig. 4A). As in previous studies [4,34], adherent cell numbers are negligible in relation to myonuclear numbers in freshly isolated mouse EDL myofibres (Fig. 4B). Unexpectedly however, most adherent cells are lost by day 5 in floating suspension, in the low-growth medium in which they were maintained. We speculate that adherent cells migrate off the surface of the myofibre into the culture medium, either remaining there or adhering to the plastic of the Petri dish. Parallel experiments, using the same media and culture conditions, in which fibres were adhered to matrigel (instead of free-floating) exhibited abundant proliferation of myoblasts beyond 5 days, suggesting that myoblasts are unlikely to undergo cell death in the suspension model. Since the contribution of adherent cell nuclei to nuclear counts is negligible, there is no significant change in myonuclear numbers throughout the time-course, thus the myonuclear domain shrinks. There remains the possibility that myonuclei apoptose and are replaced by newly proliferated myoblasts to maintain myonuclear number. To test this possibility we cultured myofibres in the constant presence of a nucleotide analogue (EdU), then at days 2 and 5 fixed and stained them for EdU and Pax7/MyoD (Fig. 4C). Co-staining with a mix of Pax7 and MyoD antibodies allowed identification of both quiescent and activated myoblasts. At day 2 a low level of labeling, just over 2 EdU positive nuclei per myofibre (Fig. 4D), was observed that by Day 5 had dropped to just 1 such nucleus among 25 myofibres, and this was positive for Pax7/MyoD. Thus there is no fusion of proliferated myoblasts to the myofibre to replace myonuclei and thus apoptosis of myonuclei is either non-existent or very rare.

Characterization of gene expression

In an effort to better understand upstream changes preceding atrophy, we measured gene expression levels, comparing freshly isolated (Day 0) myofibres with *ex vivo* cultured myofibres at Days 1 and 2. Batches of 160 myofibres, in triplicate, were collected at these time-points and mRNA was isolated. A microarray analysis identified 2061 genes that were significantly altered between Day 0 and Day 2 (Supplemental Table 1). We selected 44 of these based on their relevance to pathways of interest, and combined these with a further 12 genes of interest that had not been identified by microarray, to yield a final list of 56 genes whose mRNAs were quantified by rtPCR (Table 1).

It must be borne in mind that the *ex vivo* myofibre model includes not only the myofibre but also a small population of adherent cells (almost exclusively myoblasts), representing around 1–2% of the total nuclei, so these data require cautious interpretation. Regarding genes of which we expect a significant presence in the myofibre only, we detect downregulation of several genes associated with the contractile apparatus, including myosin heavy chain, titin, and dystrobrevin. The observed upregulation of proteasomal subunits and ubiquitinylation enzymes is in keeping with a general degradation of protein content, as measured by loss of f-actin and of total protein. Upregulation of Proteasome subunit C9 is in agreement with a previous denervation study [35]. Downstream effectors of the mTOR pathway, a putative major regulatory axis of skeletal muscle mass, are shifted to the atrophic state. The E3 ubiquitin protein ligases atrogin-1 and MuRF-1 are both upregulated by days 1 and 2, suggestive of increased protein degradation. The eukaryotic translation initiation factor 4E binding protein 1 (Eif4ebp1; also known as PHAS-1), a negative regulator of the protein initiation factor eIF-4E, is also upregulated, suggesting a suppression of protein synthesis. Akt1 and Foxo1 are upregulated and down-regulated respectively, but their activity is reported to be heavily regulated at the protein phosphorylation level, which we did not measure. The massive upregulation of tribbles homolog 3 may be relevant here since it is reported to inhibit Akt1 phosphorylation. The proteolytic gene, caspase 3 is upregulated. This is consistent with the recent demonstration that Caspase 3 is required for

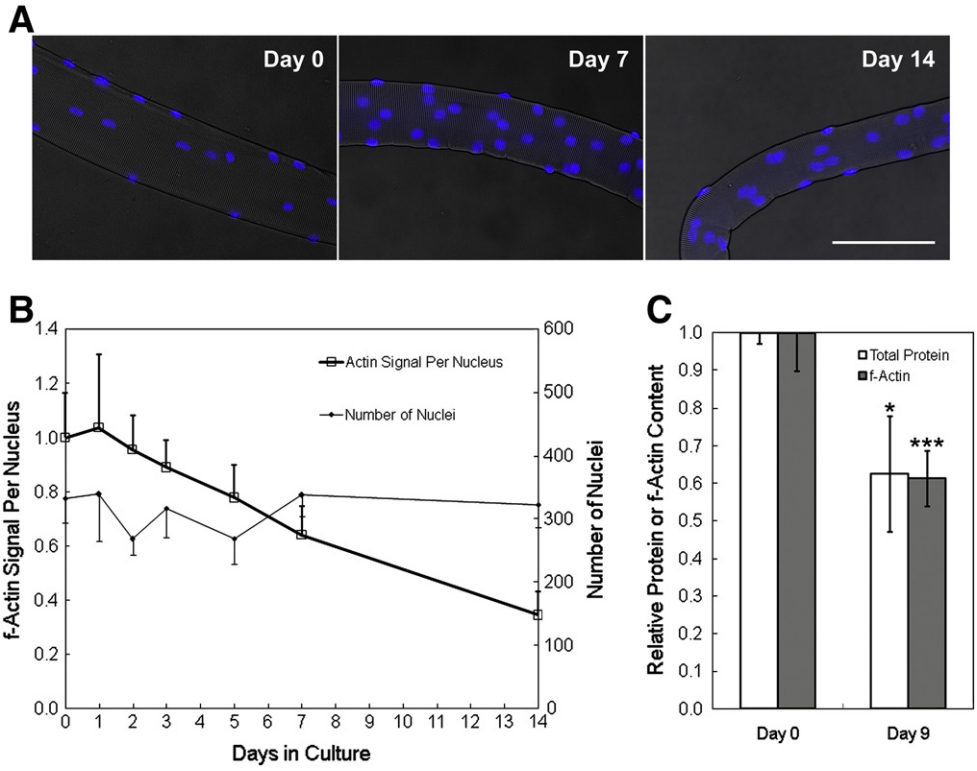

Fig. 3 – PhAct method applied to the *ex vivo* myofibre model. (A) Myofibre shrinkage during *ex vivo* culture. A representative myofibre is shown at each of day 0, 7, and 14. Each of these examples have a similar total number of nuclei. Myofibre size and distance between nuclei are observed to decrease with time. Scale bar = 100 μm. (B) f-Actin content per nucleus diminishes with time in *ex vivo* culture while nuclear number per myofibre is unchanged. Data are averages of from 7 to 21 myofibres per time-point. For clarity, 95% confidence intervals are shown in one direction only. (C) Relative f-actin content measured by PhAct is similar to relative total protein content. At days 0 and 9, the number of myofibres analyzed by PhAct was 35 and 27 respectively. Total protein was measured by quantification of silver stain intensity of SDS-PAGE-separated whole protein extracts from batches of 20 myofibres. Total protein data are averages of 4 and 7 batches (totaling 80 and 140 myofibres) at days 0 and 9 respectively. Confidence intervals (95%) are shown and *t*-test statistical significances for day 0 against day 9 are indicated (* $p<0.01$; *** $p<0.00001$).

degradation of the actinomyosin complex [36]. However, despite the association of Caspase 3 activity with apoptosis, we show (above) that apoptosis is not an observed feature of the isolated myofibre model. Another gene involved in proteolysis, Calpain 3, is downregulated, likely reflecting its regulatory role, which has been well documented post-denervation [37]. A number of other changes in mRNA expression are listed, including alteration of the NF-kB pathway, upregulation of two mitochondrial genes, perhaps because of *ex vivo* exposure to atmospheric oxygen levels, and massive downregulation of Aquaporin 4, which may be expected if adjustment is required to a subtly different osmotic environment.

The isolated myofibre as a model for testing potential modifiers of atrophy

Having established the isolated myofibre as an *ex vivo* model of atrophy, we attempted to alter the rate of atrophy by *in vitro* administration of several putative modulators of muscle mass. Various concentrations and regimes of administration were used, in which substances were added to the culture medium of the myofibres (Table 2). We observed a significant ($p<0.05$) increase in rate of atrophy with Myostatin administration at 10 ng/ml, but the effect was slight (by day 6 there was a 35% loss of f-actin as opposed to a 28% loss by untreated controls) and no change was observed at the other concentrations used (data not shown). Administration of Follistatin, contrary to naïve expectation, increased the rate of atrophy: by day 9 there was a 54% loss of f-actin as opposed to a 40% loss by untreated controls ($p<0.05$; data not shown). The rate of atrophy was unaffected by administration of Leucine at the concentrations shown.

Discussion

Ex vivo maintenance of the isolated myofibre as a model for the investigation of muscle atrophy

Since cross-sections of both healthy and atrophic skeletal muscle tissue comprise almost entirely of myofibres, muscle atrophy comes at the cost of myofibre mass. Despite the broad range of pathologies that involve muscle atrophy (recent reviews: [5,38–41]), diminution of myofibre cross-sectional area may be a universal feature. To our knowledge, a decline of myofibre number is rarely reported [42]. As well as *in vivo*, muscle atrophy has also been investigated *in vitro* using cultured myotubes. The *ex vivo*

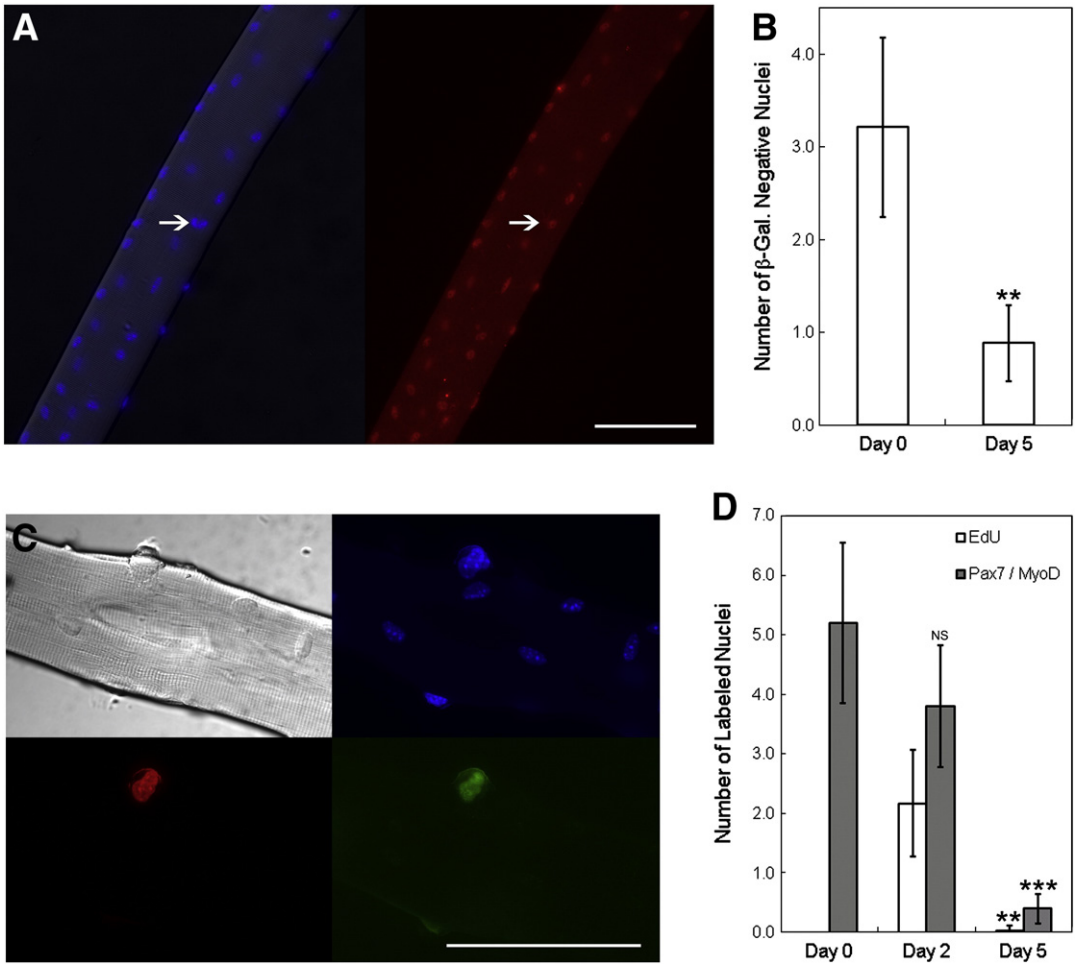

Fig. 4 – Myonuclei are not lost or replaced during *ex vivo* culture. (A) Micrographs showing DAPI-stained nuclei in blue and myofibre in brightfield (left panel) and myonuclei in red (right panel). The myofibre is isolated from a transgenic mouse exhibiting myonuclear-specific expression of β-galactosidase (β-gal), permitting labeling with antibody against β-gal. The arrow indicates the unlabeled nucleus of an adherent cell. Scale bar = 100 μm. (B) Satellite and other adherent cells are lost during *ex vivo* culture. Average numbers of β-gal negative nuclei per myofibre are shown for days 0 and 5, with 95% confidence intervals. *T*-test statistical significance is indicated for day 5 against day 0 ($p < 0.001$). Thus maintenance or increase of adherent cell number does not contribute to maintenance of nuclear number per myofibre. (C) Micrographs showing a section of a myofibre in brightfield (upper-left panel), DAPI-stained nuclei in blue (upper-right panel), and a cluster of myoblast nuclei labeled with both EdU (lower-left panel) and with an anti-Pax7/MyoD co-stain (lower-right panel). Scale bar = 100 μm. (D) Myonuclei are not replaced by proliferating myoblasts. Myofibres were cultured in the presence of the nucleotide analogue, EdU. EdU positive nuclei and nuclei positive for one or both of the myoblast markers, Pax7 and MyoD, were counted at days 0, 2, and 5. Proliferated nuclei are extremely rare by day 5 and are positive for myoblast markers. Confidence intervals (95%) are shown and *t*-test statistical significance is indicated (** $p < 0.001$; *** $p < 0.00001$, NS = not significant) for days 2 and 5 against day 0 (Pax7/MyoD) or for day 5 against day 2 (EdU).**

maintenance of myofibres described here represents an intermediate model between the *in vivo* and *in vitro* approaches, having many of the advantages of each. Prior to isolation, the myofibre has developed to full maturity in the presence of innervation, tendonal attachment, normal muscular architecture and vascularization, and the *in vivo* cytokine environment. After isolation, the myofibre loses neural stimulation and its tendinous attachments via which to perform mechanical work. It thus represents a model of disuse/denervation atrophy whose environment can be controlled on many levels including nutritional availability, oxygen potential, exposure to cytokines and to potential therapeutic compounds. Sufficient numbers of myofibres can be obtained from a single EDL muscle to allow performance of a fully internally controlled experiment, thereby reducing the number of animals to what is required to cover inter-animal variation.

The originators of the intact myofibre isolation method investigated certain physiological and morphological properties of collagen-adhered myofibres of the rat Flexor Digitorum Brevis (FDB) during several days *ex vivo*, noting various changes consistent with *in vivo* denervation, but some of which were relatively delayed [2]. We maintained myofibres of the murine EDL muscle in free-floating suspension in a 'low growth' culture medium, thereby denying a substrate for the long-term proliferation and fusion of associated myoblasts. The *ex vivo* rate of

Table 1 – List of genes showing change in mRNA levels during *ex vivo* culture of isolated myofibres. Measurements made using microarray and rtPCR methods are shown. Fold-change at day 1 or day 2 is given relative to day 0.

			Day 0 v Day 1		Day 0 v Day 2	
Category	Gene	Description	Microarray	rtPCR	Microarray	rtPCR
Proteasome	Psma1	Proteasome subunit (C2)	1.39	1.49	1.67	1.81
	Psma4	Proteasome subunit (C9)	1.15	1.60	1.71	1.66
	Psmd5	Proteasome subunit (S5B)	3.27	3.22	4.86	6.70
Ubiquitinylation	Ube1dc1	Ubiquitin-activating enzyme (E1)	4.63	6.54	4.54	7.73
	Ube2l3	Ubiquitin-conjugating enzyme (E2)	1.46	2.08	1.51	2.16
mTOR related	Akt1	Akt1		8.69		7.98
	Frap1	mTOR		1.28		1.17
	Foxo1	Forkhead box O1		−3.97		−2.87
	Fbxo32	Ubiquitin protein ligase (E3) (atrogin-1)		2.36		1.47
	Trim63	Ubiquitin protein ligase (E3) (MURF-1)		3.53		1.53
	Eif4ebp1	Eukaryotic translation initiation factor 4E binding protein 1	2.46	4.10	3.73	5.22
Structural	Actc1	Actin, alpha, cardiac	−2.10	1.09	−4.16	−1.07
	Des	Desmin		1.73		1.67
	Dtna	Dystrobrevin alpha	−2.74	−2.20	−5.02	−4.20
	Myh1	Myosin heavy chain 1	−1.41	−1.73	−1.99	−3.81
	Myom2	Myomesin 2	−1.95	1.20	−2.40	−1.38
	Tnnt2	Troponin T2, cardiac	1.06	1.69	32.32	47.43
	Tpm2	Tropomyosin 2, beta	−1.56	−1.10	−2.56	−1.39
	Ttn	Titin	−3.32	−1.85	−4.93	−3.34
	Vim	Vimentin	3.10	6.10	5.52	7.20
Proteolysis	Capn3	Calpain 3	−4.37	−3.61	−7.36	−5.29
	Casp3	Caspase 3		3.61		7.47
NF-kB related	Ikbkg	Inhibitor of kappaB kinase gamma	2.84	10.56	5.08	22.36
	Mtpn	Myotrophin	4.91	7.00	6.54	9.16
	Nfkbia	NFk light chain gene enhancer in B-cells inhibitor, alpha	2.02	3.33	1.91	3.03
	Nfkbie	NFk light polypeptide gene enhancer in B-cells inhibitor, epsilon	4.12	8.54	7.97	17.95
	Nfkbiz	NFk light polypeptide gene enhancer in B-cells inhibitor, zeta	−7.19	−2.36	−3.67	−1.01
	Plcd4	Phospholipase C, delta 4	−63.87	−23.28	−59.79	−45.43
	Tnfaip2	Tumor necrosis factor, alpha-induced protein 2	−9.98	−4.36	−5.85	−2.36
Denervation	Car3	Carbonic anhydrase 3	−1.21	1.25	−2.34	−1.23
	Ckm	Creatine kinase		1.06		−1.20
Lysosome	Ctsa	Cathepsin A	−1.79	1.24	−2.85	1.31
	Ctsc	Cathepsin C	−7.83	−2.72	−8.43	−4.17
Growth Factor	Ctgf	Connective tissue growth factor	−4.70	−10.45	−12.71	−5.33
	Igtp	Interferon gamma induced GTPase	−5.44	−5.61	−3.05	−2.28
	Iigp2	Interferon inducible GTPase 2	−6.95	−4.57	−4.64	−2.91

(continued on next page)

Table 1 (*continued*)

			Day 0 v Day 1		Day 0 v Day 2	
Category	Gene	Description	Microarray	rtPCR	Microarray	rtPCR
Anabolism	Eif2s1	Eukaryotic translation initiation factor 2, subunit 1 alpha	2.16	3.08	2.48	2.78
Remodelling	Hspa1a	Heat shock protein 1A	−29.37	−12.83	−30.57	−8.52
	Hspa1b	Heat shock protein 1B	−19.48	−12.83	−23.28	−8.52
Mitochondrial	Cat	Catalase	2.33	4.86	4.73	8.70
	Gsr	Glutathione reductase 1	2.03	22.04	4.04	50.71
	Sod1	Superoxide dismutase 1, soluble	1.10	1.23	1.35	1.36
Fibrosis	Col22a1	Collagen, type XXII, alpha 1	−5.31	−1.46	−13.71	−5.03
	Col9a1	Procollagen, type IX, alpha 1	−4.32	−1.75	−7.65	−7.20
Myogenesis	Msc	Musculin	−6.58	−8.97	−10.45	−10.05
	Myf5	Myogenic factor 5		2.77		2.84
	Myod1	Myogenic differentiation 1		−2.16		1.17
	Myog	Myogenin		3.21		33.41
	Peg3	Paternally expressed 3 (PW1)	3.05	9.89	2.93	5.71
Miscellaneous	Aqp4	Aquaporin 4	−10.21	−7.74	−51.13	−64.49
	Gsn	Gelsolin		−8.08		−2.83
	Musk	Muscle, skeletal, receptor tyrosine kinase	2.32	1.89	8.65	12.58
	Myoz1	Myozenin 1	−2.70	1.22	−5.93	−1.31
	S100a6	S100 calcium binding protein A6 (calcyclin)	2.73	5.66	14.04	18.33
	Socs3	Suppressor of cytokine signaling 3	−43.35	−24.01	−25.64	−25.10
	Trib3	Tribbles homolog 3 (Drosophila)	11.23	152.47	36.92	473.92

atrophy we observe is the same as that measured for *in vivo* denervation [6,13], tenotomization [8], and hindlimb suspension [7,10] of muscles predominant in type II myofibres. Type I myofibres can also be isolated from the soleus [3], and for those we would expect a faster rate of atrophy, as observed with *in vivo* tenotomization of the soleus [8].

The PhAct method

Fig. 5 gives a schematic overview of PhAct. Fluorescence signal from actin-bound fluorophore conjugates of the small molecule toxin, Phalloidin, is used as an index of f-actin content per myofibre. Phalloidin binds specifically to actin filaments, not to monomeric actin. In combination with counts of nuclei the f-actin content per nucleus is obtained. Plots of f-actin content against nuclear number combines the two main components of muscle fibre size into a pattern, shifts of which provide quantitative descriptors of the cellular mechanisms behind atropic and hypertropic changes wrought by a variety of treatments. Vertical displacements portray atrophy or hypertrophy generated by reduction or increase respectively in myonuclear domain. Conversely, horizontal displacements indicate changes in fibre size associated with loss or gain of myonuclear number. A major feature of this form of *ex vivo* analysis is that it can be applied to fibres that have been isolated after induction of atrophy or hypertrophy *in vivo*, and can thus be used to compare the actions of individual strategies or agents *in vivo* and *in vitro*.

Decline in f-actin content closely parallels that of total protein over nine days of myofibre *ex vivo* maintenance, suggesting that f-actin content is an accurate indicator of overall change in myofibre mass. Previous studies have used Western Blotting to measure Actin and Myosin Heavy Chain contents in various atrophic conditions *in vivo*[9,15,43–47]. Actin loss at a rate similar to or greater than Myosin Heavy Chain has been reported following denervation of mouse Gastrocnemius muscle [47] and decline of both Actin and Myosin Heavy Chain synthesis during mouse hindlimb suspension has been detected at the mRNA level after one day and the protein level after two days [9]. Actin is also lost at a similar rate to Myosin Heavy Chain in humans during bed-rest [43] and following prolonged diaphragm disuse [44]. However, one study described a two-fold faster decline of Myosin Heavy Chain than Actin following rat spinal cord isolation [48], and early loss of Actin without loss of MHC is observed *in vitro* following 32 hour treatment of cultured myotubes with dexamethasone [15]. Myosin Heavy Chain has been described to decline without any loss of Actin during cachexia [45], Application of the PhAct method should determine whether differences exist in the quantitative characteristics of actin loss between forms of atrophy such as cachexia. Other indicators of the importance of actin content

Table 2 – Effects of several putative modifiers of muscle mass on rate of atrophy.

Molecule	Concentration(s)	Regime	Effect on rate of atrophy
Myostatin	10 ng/ml, 100 ng/ml, 500 ng/ml	Every 3 days for 6 days	↑ (at 10 ng/ml)
Follistatin	100 ng/ml	Every 3 days for 9 days	↑
Leucine	0.2 mM, 5 mM, 10 mM	Every 3 days for 6 days	None detected

in the context of muscle mass are that actin synthesis is decreased with age in rats [46] and that actin mRNA levels and protein synthesis rate recover quickly on muscle reloading following hindlimb suspension in rats [49].

The PhAct method is suitable for general application to small animal models of muscle growth and disease, where it is of interest to assay the effects of *in vivo* treatments and interventions. The method is sensitive and convenient, since the isolation of myofibres is now a routine tool of the field. It has the advantage over existing approaches of providing information at the cellular (per myofibre) level. Existing approaches to the assay of change in muscle mass *in vivo* are limited to coarse measurement of whole muscle weight and protein content [6–9] or to indirect inferences from muscle cross-sections [10–12]. The major alternative, myotube tissue cultures, are valuable for analysis of molecular mechanisms but of questionable relevance to control of muscle size *in vivo*[14–16]. One recent study describes estimation of isolated myofibre volume using standard microscopy equipment [33] by a combination of cross-sectional data with measurements of myofibre length but does not provide information on protein

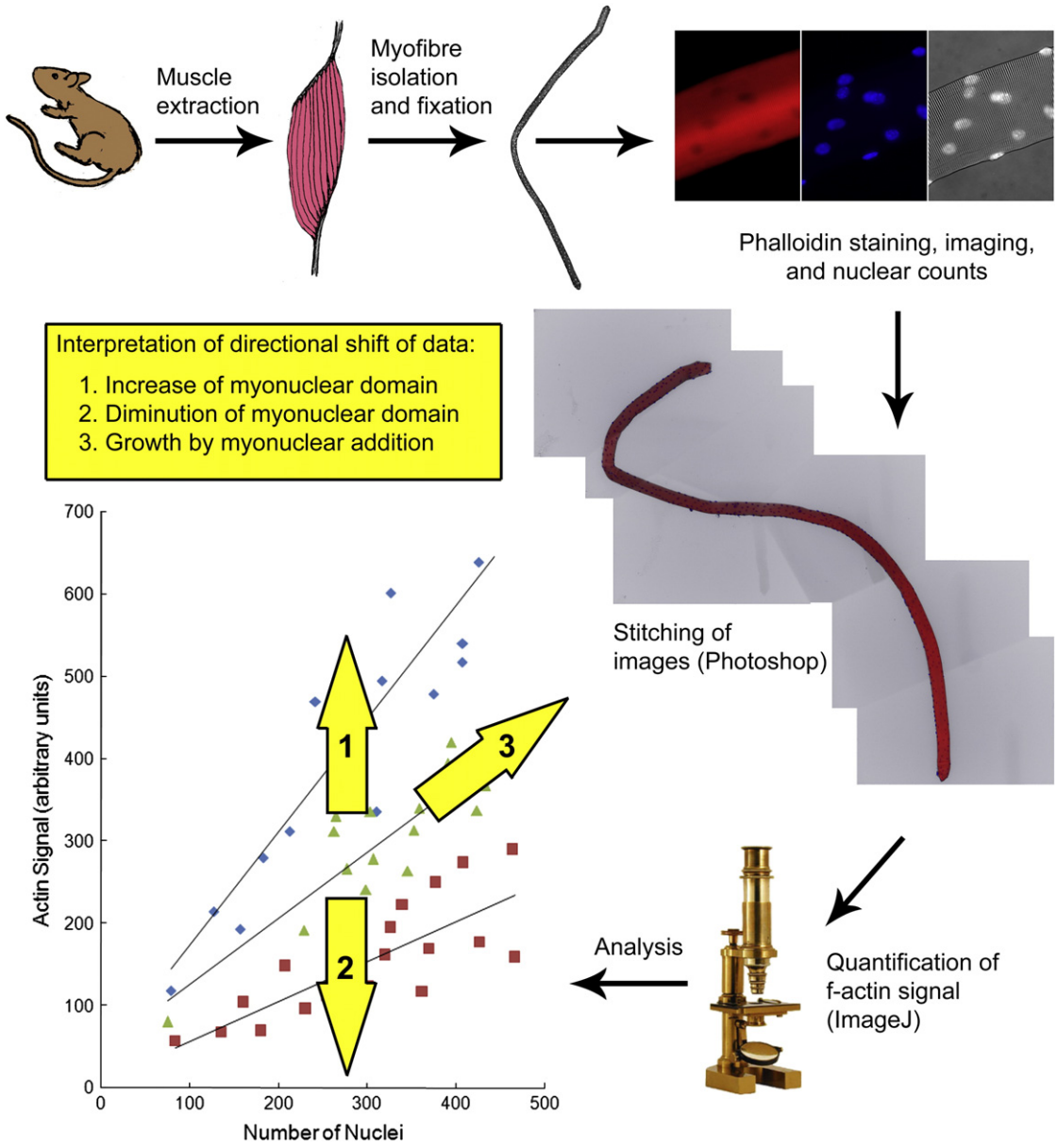

Fig. 5 – Schematic overview of the PhAct method with explanation of how data may be interpreted.

content. Measurement of cross-sectional area per myofibre is the most common approach to the assay of change in muscle mass at a cellular level, but it is prone to inaccuracies due to the orientation of the muscle during sectioning, and takes no account of myofibre length.

Ex vivo myofibre atrophy occurs without loss or replacement of myonuclei

Since we observe a decreased size and protein content of myofibres following *ex vivo* maintenance but with no loss or replacement of myonuclei we conclude that the myonuclear domain is diminished and that myonuclear apoptosis is either absent or rare. We find that myofibres of the predominantly 'fast' EDL muscle show very similar rates of actin and total protein loss during *ex vivo* maintenance to *in vivo* models of denervation [6,13], tenotomization [8], and hindlimb suspension [7,10]. In one such study, time-lapse microscopy was used to demonstrate loss of cross-sectional area without loss of myonuclei over several weeks of *in vivo* denervation of the EDL and Soleus muscles [13]. These findings are consistent with reports of fast-twitch myofibre atrophy without detectable myonuclear loss in various contexts, such as denervation of rat diaphragm [17], denervation of plantaris muscles of mature mice (although some myonuclear loss was seen in myofibres of young mice) [18], of rat plantaris after spinal cord transection [27], of rat Soleus after spinal cord isolation [19], of rat Soleus and Plantaris muscles after 28-day hindlimb suspension [20], and short-term spaceflight induced atrophy of the Soleus muscle of the Rat [21,24] and the Rhesus monkey [22] and of Rat Tibialis Anterior and Gastrocnemius [23]. These findings support the paradigm that inactivation-induced atrophy occurs primarily via diminution of the myonuclear domain, and does not require myonuclear apoptosis, at least in the case of fast-twitch myofibres.

Several studies report loss of myonuclei and/or increased apoptosis in situations of atrophy or reduced functional demand [24–27,50–52] (reviewed here [53]). Exclusively this is reported for slow-twitch myofibres in environments featuring a transition from type I to type II MHC expression such as occurs in the Soleus muscle during hindlimb suspension [26,54] and spaceflight [24]. Fast-twitch myofibres have fewer nuclei than slow-twitch, and spinal isolation has been associated with the appearance of fast-twitch myofibres that may have switched fibre type and undergone significant myonuclear loss [25]. One study reports no loss of myonuclei despite massive Soleus myofibre atrophy following Rat spinal cord isolation [19]. Regardless of the extent to which myonuclei are lost and whether fibre-type switching is involved, atrophy of slow-twitch myofibres likely involves a diminution of the myonuclear domain, since the reported loss of cytoplasmic volume is usually disproportionate to the loss of myonuclei [19,24–26].

A number of studies [25,55–60] report increased myonuclear numbers in various myofibre types when functional demand is increased, and in this context there is a commensurate change in cytoplasmic volume such that myonuclear domain size is maintained. This commensurate change may not be simultaneous, but reports are conflicting over which occurs first. A recent report shows myonuclear accretion to precede the occurrence of hypertrophy in response to increased functional demand in the mouse EDL [60] but this appears contradictory to findings in overloaded rat Plantaris [61]. Thus diminution of the myonuclear domain may be the primary response to inactivity and disuse, since myonuclear loss need not precede muscle atrophy, but size of the myonuclear domain is maintained following muscle hypertrophy.

Characterization of early changes in gene expression in the ex vivo myofibre atrophy model

Atrophy-associated changes to whole muscle gene expression have been characterized in small mammals [62–66] and humans [67–70], and are generally consistent with the putative designation of the E3 ubiquitin protein ligases as the primary down-stream effectors of myofibre shrinkage [63]. Models of associated signaling pathways have been proposed (reviewed [38,40,41]). The present study is the first to profile mRNA expression of only the myofibre with its associated satellite cells, eliminating vasculature and other interstitial tissue that may confound gene expression analyses. We measured changes occurring over the first 48 hours of single myofibre *ex vivo* maintenance. Microarray profiling identified 2061 significantly altered genes and an overlapping set of 56 mRNAs were quantified by rtPCR. The observed changes were consistent with increased proteolytic and proteasomal activity, including upregulation of the E3 ubiquitin protein ligases atrogin-1 and MuRF-1, upregulation of Eif4ebp1, a negative regulator of the protein initiation factor eIF-4E, and downregulation of major contractile components such as Myosin Heavy Chain and Titin. These data serve as a baseline for comparison against future manipulations of the *ex vivo* myofibre maintenance model, such as to test whether anti-atrophic compounds affect mRNA levels.

Influences of cytokines on the rate of ex vivo atrophy

Since the identification of Myostatin as an important negative regulator of muscle mass [28] much effort has gone into the identification of means to block its activity, such as via the inhibitory glycoprotein, Follistatin (for review see [71]). We detect a small increase in rate of atrophy with the addition of Myostatin at 10 ng/ml but not at 100 or 500 ng/ml. This is suggestive of a bimodal response, which has not been noted previously [72,73]. Recently it has been shown that *in vivo* muscle hypertrophy induced by myostatin blockade occurs without a rise in myonuclear number, indicating that myoblast fusion is not required [74], despite observations of myoblast behavioural regulation by high concentrations of myostatin [75–78]. Questions such as this can now be more sensitively resolved by measuring subtle *in vivo* change to muscle mass using the PhAct method. Our method of quantitative analyses of myonuclear number and fibrous actin content can be applied directly to muscle fibres isolated after *in vivo* atrophic and hypertrophic treatments. It should prove a useful tool in disentangling effects directly on the muscle fibre, from those that are mediated by various *in vivo* interactions. Interestingly, and contrary to expectation, Follistatin administration also increased the rate of atrophy in our isolated fibre preparations, a marked contrast to its reported action *in vivo*[29,79], that merits further investigation.

This work establishes the *ex vivo* myofibre as a suitable model for the testing of potential modifiers of atrophy, such as screening of compounds for their anti-atrophic properties. Its principal limitations arise from both practical and theoretical causes. Practically, it is effectively limited to muscles from which we can dissociate single fibres. Some problems of interpretation may arise where the muscle consists of very disparate populations of muscle

fibres, e.g. the tibialis anterior where the superficial and deep regions differ significantly from one another. The usefulness of the technique would also be improved if we were able to reliably distinguish fibre types; up to now, our attempts to do so by immunostaining for myosin heavy chain isoforms have been foiled by high background signal, but we would expect that this will be resolved by technical refinement. As it stands, this protocol would not easily transfer between laboratories because of the arbitrary normalization of fluorescent signal to a standard concentration of fluorescent phalloidin. However, calibration to a primary reference, such as a known concentration of fibrous actin protein in agar would facilitate comparisons between individual studies.

Balanced against these problems is the fact that the isolated fibre protocol presents us with an experimentally accessible model of muscle atrophy as it applies to mature muscle fibers, that can be used to pick apart the mechanisms behind the control of muscle size and of treatments and agents that mediate this control. To advance work in this topic from its current largely empirical status we need to gather information on mechanisms at the cellular as well as the molecular levels of organization. It will be of interest, for example, to examine combined administrations of Myostatin and Follistatin both *in vivo* and in our *ex vivo* system and to compare the cellular responses as well as the early gene expression changes they induce in each case.

Supplementary materials related to this article can be found online at doi:10.1016/j.yexcr.2011.05.013.

Acknowledgment

This work was partially supported by NIH NCMRR/NINDS 5R24 HD050846 (Integrated Molecular Core for Rehabilitation Medicine).

REFERENCES

[1] A. Bekoff, W.J. Betz, Physiological properties of dissociated muscle fibres obtained from innervated and denervated adult rat muscle, J. Physiol. 271 (1977) 25–40.
[2] A. Bekoff, W. Betz, Properties of isolated adult rat muscle fibres maintained in tissue culture, J. Physiol. 271 (1977) 537–547.
[3] J.D. Rosenblatt, A.I. Lunt, D.J. Parry, T.A. Partridge, Culturing satellite cells from living single muscle fiber explants, In Vitro Cell Dev. Biol. Anim. 31 (1995) 773–779.
[4] C.A. Collins, I. Olsen, P.S. Zammit, L. Heslop, A. Petrie, T.A. Partridge, J.E. Morgan, Stem cell function, self-renewal, and behavioral heterogeneity of cells from the adult muscle satellite cell niche, Cell 122 (2005) 289–301.
[5] M.J. Tisdale, The ubiquitin-proteasome pathway as a therapeutic target for muscle wasting, J. Support. Oncol. 3 (2005) 209–217.
[6] R.T. Hinkle, E. Donnelly, D.B. Cody, M.B. Bauer, R.J. Isfort, Urocortin II treatment reduces skeletal muscle mass and function loss during atrophy and increases nonatrophying skeletal muscle mass and function, Endocrinology 144 (2003) 4939–4946.
[7] C.A. Morris, L.D. Morris, A.R. Kennedy, H.L. Sweeney, Attenuation of skeletal muscle atrophy via protease inhibition, J. Appl. Physiol. 99 (2005) 1719–1727.
[8] A. Jakubiec-Puka, C. Catani, U. Carraro, Myosin heavy-chain composition in striated muscle after tenotomy, Biochem. J. 282 (Pt 1) (1992) 237–242.
[9] J.M. Giger, P.W. Bodell, M. Zeng, K.M. Baldwin, F. Haddad, Rapid muscle atrophy response to unloading: pretranslational processes involving MHC and actin, J. Appl. Physiol. 107 (2009) 1204–1212.
[10] J. Eash, A. Olsen, G. Breur, D. Gerrard, K. Hannon, FGFR1 inhibits skeletal muscle atrophy associated with hindlimb suspension, BMC Musculoskelet. Disord. 8 (2007) 32.
[11] S.J. Lee, Quadrupling muscle mass in mice by targeting TGF-beta signaling pathways, PLoS One 2 (2007) e789.
[12] M.E. Cleasby, T.A. Reinten, G.J. Cooney, D.E. James, E.W. Kraegen, Functional studies of Akt isoform specificity in skeletal muscle in vivo; maintained insulin sensitivity despite reduced insulin receptor substrate-1 expression, Mol. Endocrinol. 21 (2007) 215–228.
[13] J.C. Bruusgaard, K. Gundersen, In vivo time-lapse microscopy reveals no loss of murine myonuclei during weeks of muscle atrophy, J. Clin. Invest. 118 (2008) 1450–1457.
[14] Y.P. Li, R.J. Schwartz, I.D. Waddell, B.R. Holloway, M.B. Reid, Skeletal muscle myocytes undergo protein loss and reactive oxygen-mediated NF-kappaB activation in response to tumor necrosis factor alpha, FASEB J. 12 (1998) 871–880.
[15] B.A. Clarke, D. Drujan, M.S. Willis, L.O. Murphy, R.A. Corpina, E. Burova, S.V. Rakhilin, T.N. Stitt, C. Patterson, E. Latres, D.J. Glass, The E3 Ligase MuRF1 degrades myosin heavy chain protein in dexamethasone-treated skeletal muscle, Cell Metab. 6 (2007) 376–385.
[16] W. Li, J.S. Moylan, M.A. Chambers, J. Smith, M.B. Reid, Interleukin-1 stimulates catabolism in C2C12 myotubes, Am. J. Physiol. Cell Physiol. 297 (2009) C706–C714.
[17] B. Aravamudan, C.B. Mantilla, W.Z. Zhan, G.C. Sieck, Denervation effects on myonuclear domain size of rat diaphragm fibers, J. Appl. Physiol. 100 (2006) 1617–1622.
[18] K.I. Wada, H. Takahashi, S. Katsuta, H. Soya, No decrease in myonuclear number after long-term denervation in mature mice, Am. J. Physiol. Cell Physiol. 283 (2002) C484–C488.
[19] H. Zhong, R.R. Roy, B. Siengthai, V.R. Edgerton, Effects of inactivity on fiber size and myonuclear number in rat soleus muscle, J. Appl. Physiol. 99 (2005) 1494–1499.
[20] C.E. Kasper, L. Xun, Cytoplasm-to-myonucleus ratios in plantaris and soleus muscle fibres following hindlimb suspension, J. Muscle Res. Cell Motil. 17 (1996) 603–610.
[21] R.S. Hikida, S. Van Nostran, J.D. Murray, R.S. Staron, S.E. Gordon, W.J. Kraemer, Myonuclear loss in atrophied soleus muscle fibers, Anat. Rec. 247 (1997) 350–354.
[22] R.R. Roy, H. Zhong, R.J. Talmadge, S.C. Bodine, J.W. Fanton, I. Koslovskaya, V.R. Edgerton, Size and myonuclear domains in Rhesus soleus muscle fibers: short-term spaceflight, J. Gravit. Physiol. 8 (2001) 49–56.
[23] C.E. Kasper, L. Xun, Cytoplasm-to-myonucleus ratios following microgravity, J. Muscle Res. Cell Motil. 17 (1996) 595–602.
[24] D.L. Allen, W. Yasui, T. Tanaka, Y. Ohira, S. Nagaoka, C. Sekiguchi, W.E. Hinds, R.R. Roy, V.R. Edgerton, Myonuclear number and myosin heavy chain expression in rat soleus single muscle fibers after spaceflight, J. Appl. Physiol. 81 (1996) 145–151.
[25] D.L. Allen, S.R. Monke, R.J. Talmadge, R.R. Roy, V.R. Edgerton, Plasticity of myonuclear number in hypertrophied and atrophied mammalian skeletal muscle fibers, J. Appl. Physiol. 78 (1995) 1969–1976.
[26] Y. Oishi, T. Ogata, K.I. Yamamoto, M. Terada, T. Ohira, Y. Ohira, K. Taniguchi, R.R. Roy, Cellular adaptations in soleus muscle during recovery after hindlimb unloading, Acta Physiol. (Oxf) 192 (2008) 381–395.
[27] E.E. Dupont-Versteegden, R.J. Murphy, J.D. Houle, C.M. Gurley, C.A. Peterson, Mechanisms leading to restoration of muscle size with exercise and transplantation after spinal cord injury, Am. J. Physiol. Cell Physiol. 279 (2000) C1677–C1684.
[28] A.C. McPherron, A.M. Lawler, S.J. Lee, Regulation of skeletal muscle mass in mice by a new TGF-beta superfamily member, Nature 387 (1997) 83–90.
[29] S.J. Lee, A.C. McPherron, Regulation of myostatin activity and muscle growth, Proc. Natl. Acad. Sci. U. S. A. 98 (2001) 9306–9311.
[30] A. Philippou, A. Halapas, M. Maridaki, M. Koutsilieris, Type I insulin-like growth factor receptor signaling in skeletal muscle

regeneration and hypertrophy, J. Musculoskelet. Neuronal Interact. 7 (2007) 208–218.
[31] J.C. Anthony, T.G. Anthony, D.K. Layman, Leucine supplementation enhances skeletal muscle recovery in rats following exercise, J. Nutr. 129 (1999) 1102–1106.
[32] R. Kelly, S. Alonso, S. Tajbakhsh, G. Cossu, M. Buckingham, Myosin light chain 3 F regulatory sequences confer regionalized cardiac and skeletal muscle expression in transgenic mice, J. Cell Biol. 129 (1995) 383–396.
[33] R.B. White, A.S. Bierinx, V.F. Gnocchi, P.S. Zammit, Dynamics of muscle fibre growth during postnatal mouse development, BMC Dev. Biol. 10 (2010) 21.
[34] P.S. Zammit, L. Heslop, V. Hudon, J.D. Rosenblatt, S. Tajbakhsh, M.E. Buckingham, J.R. Beauchamp, T.A. Partridge, Kinetics of myoblast proliferation show that resident satellite cells are competent to fully regenerate skeletal muscle fibers, Exp. Cell Res. 281 (2002) 39–49.
[35] R. Medina, S.S. Wing, A.L. Goldberg, Increase in levels of polyubiquitin and proteasome mRNA in skeletal muscle during starvation and denervation atrophy, Biochem. J. 307 (Pt 3) (1995) 631–637.
[36] P.J. Plant, J.R. Bain, J.E. Correa, M. Woo, J. Batt, Absence of caspase-3 protects against denervation-induced skeletal muscle atrophy, J. Appl. Physiol. 107 (2009) 224–234.
[37] D. Stockholm, M. Herasse, S. Marchand, C. Praud, C. Roudaut, I. Richard, A. Sebille, J.S. Beckmann, Calpain 3 mRNA expression in mice after denervation and during muscle regeneration, Am. J. Physiol. Cell Physiol. 280 (2001) C1561–C1569.
[38] M.J. Tisdale, Is there a common mechanism linking muscle wasting in various disease types? Curr. Opin. Support. Palliat. Care 1 (2007) 287–292.
[39] T.P. Stein, D.R. Bolster, Insights into muscle atrophy and recovery pathway based on genetic models, Curr. Opin. Clin. Nutr. Metab. Care 9 (2006) 395–402.
[40] M. Sandri, Signaling in muscle atrophy and hypertrophy, Physiology (Bethesda) 23 (2008) 160–170.
[41] D.J. Glass, Skeletal muscle hypertrophy and atrophy signaling pathways, Int. J. Biochem. Cell Biol. 37 (2005) 1974–1984.
[42] C.K. Daw, J.W. Starnes, T.P. White, Muscle atrophy and hypoplasia with aging: impact of training and food restriction, J. Appl. Physiol. 64 (1988) 2428–2432.
[43] E. Borina, M.A. Pellegrino, G. D'Antona, R. Bottinelli, Myosin and actin content of human skeletal muscle fibers following 35 days bed rest, Scand. J. Med. Sci. Sports 20 (2010) 65–73.
[44] S. Levine, C. Biswas, J. Dierov, R. Barsotti, J.B. Shrager, T. Nguyen, S. Sonnad, J.C. Kucharchzuk, L.R. Kaiser, S. Singhal, M.T. Budak, Increased proteolysis myosin depletion and atrophic AKT-FOXO signaling in human diaphragm disuse, Am. J. Respir. Crit. Care Med. 183 (2010) 483–490.
[45] S. Acharyya, K.J. Ladner, L.L. Nelsen, J. Damrauer, P.J. Reiser, S. Swoap, D.C. Guttridge, Cancer cachexia is regulated by selective targeting of skeletal muscle gene products, J. Clin. Invest. 114 (2004) 370–378.
[46] P. Kaasik, M. Umnova, A. Pehme, K. Alev, M. Aru, A. Selart, T. Seene, Ageing and dexamethasone associated sarcopenia: peculiarities of regeneration, J. Steroid Biochem. Mol. Biol. 105 (2007) 85–90.
[47] S. Cohen, J.J. Brault, S.P. Gygi, D.J. Glass, D.M. Valenzuela, C. Gartner, E. Latres, A.L. Goldberg, During muscle atrophy, thick, but not thin, filament components are degraded by MuRF1-dependent ubiquitylation, J. Cell Biol. 185 (2009) 1083–1095.
[48] F. Haddad, R.R. Roy, H. Zhong, V.R. Edgerton, K.M. Baldwin, Atrophy responses to muscle inactivity. I. Cellular markers of protein deficits, J. Appl. Physiol. 95 (2003) 781–790.
[49] P.R. Morrison, G.W. Muller, F.W. Booth, Actin synthesis rate and mRNA level increase during early recovery of atrophied muscle, Am. J. Physiol. 253 (1987) C205–C209.
[50] D.L. Allen, J.K. Linderman, R.R. Roy, A.J. Bigbee, R.E. Grindeland, V. Mukku, V.R. Edgerton, Apoptosis: a mechanism contributing to remodeling of skeletal muscle in response to hindlimb unweighting, Am. J. Physiol. 273 (1997) C579–C587.
[51] E.E. Dupont-Versteegden, R.J. Murphy, J.D. Houle, C.M. Gurley, C.A. Peterson, Activated satellite cells fail to restore myonuclear number in spinal cord transected and exercised rats, Am. J. Physiol. 277 (1999) C589–C597.
[52] J.C. Gallegly, N.A. Turesky, B.A. Strotman, C.M. Gurley, C.A. Peterson, E.E. Dupont-Versteegden, Satellite cell regulation of muscle mass is altered at old age, J. Appl. Physiol. 97 (2004) 1082–1090.
[53] E.E. Dupont-Versteegden, Apoptosis in skeletal muscle and its relevance to atrophy, World J. Gastroenterol. 12 (2006) 7463–7466.
[54] Y. Oishi, A. Ishihara, H. Yamamoto, E. Miyamoto, Hindlimb suspension induces the expression of multiple myosin heavy chain isoforms in single fibres of the rat soleus muscle, Acta Physiol. Scand. 162 (1998) 127–134.
[55] J.K. Petrella, J.S. Kim, D.L. Mayhew, J.M. Cross, M.M. Bamman, Potent myofiber hypertrophy during resistance training in humans is associated with satellite cell-mediated myonuclear addition: a cluster analysis, J. Appl. Physiol. 104 (2008) 1736–1742.
[56] R.S. Hikida, R.S. Staron, F.C. Hagerman, S. Walsh, E. Kaiser, S. Shell, S. Hervey, Effects of high-intensity resistance training on untrained older men. II. Muscle fiber characteristics and nucleo-cytoplasmic relationships, J. Gerontol. A Biol. Sci. Med. Sci. 55 (2000) B347–B354.
[57] F. Kadi, L.E. Thornell, Concomitant increases in myonuclear and satellite cell content in female trapezius muscle following strength training, Histochem. Cell Biol. 113 (2000) 99–103.
[58] R.R. Roy, S.R. Monke, D.L. Allen, V.R. Edgerton, Modulation of myonuclear number in functionally overloaded and exercised rat plantaris fibers, J. Appl. Physiol. 87 (1999) 634–642.
[59] F. Kadi, A. Eriksson, S. Holmner, G.S. Butler-Browne, L.E. Thornell, Cellular adaptation of the trapezius muscle in strength-trained athletes, Histochem. Cell Biol. 111 (1999) 189–195.
[60] J.C. Bruusgaard, I.B. Johansen, I.M. Egner, Z.A. Rana, K. Gundersen, Myonuclei acquired by overload exercise precede hypertrophy and are not lost on detraining, Proc. Natl. Acad. Sci. U. S. A. 107 (2010) 15111–15116.
[61] S.F. van der Meer, R.T. Jaspers, D.A. Jones, H. Degens, The time course of myonuclear accretion during hypertrophy in young adult and older rat plantaris muscle, Ann. Anat. 193 (2010) 56–63.
[62] S.C. Bodine, T.N. Stitt, M. Gonzalez, W.O. Kline, G.L. Stover, R. Bauerlein, E. Zlotchenko, A. Scrimgeour, J.C. Lawrence, D.J. Glass, G.D. Yancopoulos, Akt/mTOR pathway is a crucial regulator of skeletal muscle hypertrophy and can prevent muscle atrophy in vivo, Nat. Cell Biol. 3 (2001) 1014–1019.
[63] S.C. Bodine, E. Latres, S. Baumhueter, V.K. Lai, L. Nunez, B.A. Clarke, W.T. Poueymirou, F.J. Panaro, E. Na, K. Dharmarajan, Z.Q. Pan, D.M. Valenzuela, T.M. DeChiara, T.N. Stitt, G.D. Yancopoulos, D.J. Glass, Identification of ubiquitin ligases required for skeletal muscle atrophy, Science 294 (2001) 1704–1708.
[64] A.M. Ahtikoski, S.O. Koskinen, P. Virtanen, V. Kovanen, J. Risteli, T.E. Takala, Synthesis and degradation of type IV collagen in rat skeletal muscle during immobilization in shortened and lengthened positions, Acta. Physiol. Scand. 177 (2003) 473–481.
[65] L. Bey, N. Akunuri, P. Zhao, E.P. Hoffman, D.G. Hamilton, M.T. Hamilton, Patterns of global gene expression in rat skeletal muscle during unloading and low-intensity ambulatory activity, Physiol. Genomics 13 (2003) 157–167.
[66] S.H. Lecker, R.T. Jagoe, A. Gilbert, M. Gomes, V. Baracos, J. Bailey, S.R. Price, W.E. Mitch, A.L. Goldberg, Multiple types of skeletal muscle atrophy involve a common program of changes in gene expression, FASEB J. 18 (2004) 39–51.
[67] Y.W. Chen, C.M. Gregory, M.T. Scarborough, R. Shi, G.A. Walter, K. Vandenborne, Transcriptional pathways associated with skeletal muscle disuse atrophy in humans, Physiol. Genomics 31 (2007) 510–520.
[68] S.W. Jones, R.J. Hill, P.A. Krasney, B. O'Conner, N. Peirce, P.L. Greenhaff, Disuse atrophy and exercise rehabilitation in humans profoundly affects the expression of genes associated with the regulation of skeletal muscle mass, FASEB J. 18 (2004) 1025–1027.

[69] M.L. Urso, A.G. Scrimgeour, Y.W. Chen, P.D. Thompson, P.M. Clarkson, Analysis of human skeletal muscle after 48 h immobilization reveals alterations in mRNA and protein for extracellular matrix components, J. Appl. Physiol. 101 (2006) 1136–1148.
[70] K.A. Reich, Y.W. Chen, P.D. Thompson, E.P. Hoffman, P.M. Clarkson, 48 hours of unloading and 24 hours of reloading leads to changes in global gene expression patterns related to ubiquitination and oxidative stress in humans, J. Appl. Physiol. 109 (2010) 1404–1415.
[71] L.R. Rodino-Klapac, A.M. Haidet, J. Kota, C. Handy, B.K. Kaspar, J.R. Mendell, Inhibition of myostatin with emphasis on follistatin as a therapy for muscle disease, Muscle Nerve 39 (2009) 283–296.
[72] W.E. Taylor, S. Bhasin, J. Artaza, F. Byhower, M. Azam, D.H. Willard Jr., F.C. Kull Jr., N. Gonzalez-Cadavid, Myostatin inhibits cell proliferation and protein synthesis in C2C12 muscle cells, Am. J. Physiol. Endocrinol. Metab. 280 (2001) E221–E228.
[73] P. Ciarmela, E. Wiater, S.M. Smith, W. Vale, Presence, actions, and regulation of myostatin in rat uterus and myometrial cells, Endocrinology 150 (2009) 906–914.
[74] H. Amthor, A. Otto, A. Vulin, A. Rochat, J. Dumonceaux, L. Garcia, E. Mouisel, C. Hourde, R. Macharia, M. Friedrichs, F. Relaix, P.S. Zammit, A. Matsakas, K. Patel, T. Partridge, Muscle hypertrophy driven by myostatin blockade does not require stem/precursor-cell activity, Proc. Natl. Acad. Sci. U. S. A. 106 (2009) 7479–7484.
[75] M. Thomas, B. Langley, C. Berry, M. Sharma, S. Kirk, J. Bass, R. Kambadur, Myostatin, a negative regulator of muscle growth, functions by inhibiting myoblast proliferation, J. Biol. Chem. 275 (2000) 40235–40243.
[76] B. Langley, M. Thomas, A. Bishop, M. Sharma, S. Gilmour, R. Kambadur, Myostatin inhibits myoblast differentiation by down-regulating MyoD expression, J. Biol. Chem. 277 (2002) 49831–49840.
[77] S. McCroskery, M. Thomas, L. Maxwell, M. Sharma, R. Kambadur, Myostatin negatively regulates satellite cell activation and self-renewal, J. Cell Biol. 162 (2003) 1135–1147.
[78] S. McCroskery, M. Thomas, L. Platt, A. Hennebry, T. Nishimura, L. McLeay, M. Sharma, R. Kambadur, Improved muscle healing through enhanced regeneration and reduced fibrosis in myostatin-null mice, J. Cell Sci. 118 (2005) 3531–3541.
[79] A.M. Haidet, L. Rizo, C. Handy, P. Umapathi, A. Eagle, C. Shilling, D. Boue, P.T. Martin, Z. Sahenk, J.R. Mendell, B.K. Kaspar, Long-term enhancement of skeletal muscle mass and strength by single gene administration of myostatin inhibitors, Proc. Natl. Acad. Sci. U. S. A. 105 (2008) 4318–4322.